

# JOURNAL OF MECHANICS OF CONTINUA AND MATHEMATICAL SCIENCES

www.journalimcms.org



ISSN (Online): 2454-7190 Vol.-20, No.-11, November (2025) pp 91-101 ISSN (Print) 0973-8975

# RESEARCH OF CHARACTERISTICS OF THE BATTERY USED ON HYBRID VEHICLES

Lam Kim Thanh Vo<sup>1</sup>, Xuan Ngoc Nguyen<sup>2</sup>, Hong Phuc Vo<sup>3</sup>, Tien Phuc Dang<sup>4</sup>, Khoi Nguyen Nguyen<sup>5</sup>, Thanh Tam Tran<sup>6</sup>

<sup>1,2,3,4,5</sup> Faculty of Automotive Engineering Technology, Industrial University of Ho Chi Minh City, Ho Chi Minh City 700000, Vietnam.

<sup>6</sup>Faculty of Electrics - Electronics, Thu Duc College of Technology, Ho Chi Minh City 700000, Vietnam.

Email: <sup>1</sup>volamkimthanh@iuh.edu.vn, <sup>2</sup>nguyenxuanngoc@iuh.edu.vn <sup>3</sup>21036381.phuc@student.iuh.edu.vn, <sup>4</sup>dangtienphuc@iuh.edu.vn <sup>5</sup>nguyenkhoinguyen@iuh.edu.vn, <sup>6</sup>tranthanhtam@tdc.edu.vn

Corresponding Author: Xuan Ngoc Nguyen

https://doi.org/10.26782/jmcms.2025.11.00006

(Received: August 25, 2025; Revised: October 12, 2025; November 06, 2025)

#### **Abstract**

The fount of battery in a hybrid automobile plays an important role in furnishing energy to sustain the seamless functionality of the vehicle and mitigate petroleum expenditure. This power source is mostly used as a collection of many cells combined into a single power source for the vehicle. This research concentrates on considering the charging attributes of the battery supplied in a hybrid automobile, encompassing charging flow, the state of charge (SoC), and the charging environment thermal influence on the efficacy of the battery power. Matlab Simulink software is applied to investigate and simulate the characteristic curves of the above factors to propose effective ways to use batteries in hybrid vehicles. The results of the article are used as basic knowledge for researching the battery, and at the same time serve the development of batteries for electric vehicles in the future.

Keywords: Charging time, Battery, Hybrid, Matlab Simulink, Pin Ni-MH.

#### **Nomenclature**

 $\begin{array}{ll} U_{pack} & Total \ voltage \ of \ the \ battery \ pack, \ V \\ N_{Module} & Total \ number \ of \ modules \ in \ a \ battery \ pack \\ U_{Module} & The \ voltage \ of \ the \ module \ in \ the \ battery, \ V \end{array}$ 

C<sub>pack</sub> Capacity of battery pack, Ah

 $P_{Theory}$  The power of the supplied battery pack, kW R The internal resistance of the battery,  $\Omega$ 

 $E_{Module}$  The energy of the battery, Wh

 $C_{Module}$  The capacity of the module in battery, Ah  $m_{Module}$  The mass of the module in the battery, Kg

E<sub>Sp-Module</sub> The specific energy of the module in the battery, Wh.Kg<sup>-1</sup>

E<sub>pack</sub> The energy of the battery pack, Wh

P The power of the supplied battery pack, kW

P<sub>Loss</sub> The loss of power, kW

I The current intensity of the battery, A  $V_{OC}$  Open circuit voltage of the battery, V

SoC(t) Charging status at time t, %

$$\begin{split} S_{0}C_{0} & \text{Initial charging status at the time } t_{0} = 0\% \\ C_{nom} & \text{Nominal capacity of the battery, Ah} \\ I_{bat(t)} & \text{Current intensity (Fast charging cable), A} \\ I_{batt} & \text{Current intensity (Standard charging line), A} \end{split}$$

$$\begin{split} &I_{ef} & & Effective \ current, \ A \\ &Q & & The \ stored \ charge, \ Ah \\ &t_{Standard} & Standard \ charging \ time, \ h \\ &t_{Fast} & Fast \ charging \ time, \ h \end{split}$$

#### **Greek Symbols**

η Charging efficiency, %

 $\Delta_{\rm t}$  Time of each stage

#### I. Introduction

Nowadays, the proportion of electric vehicle users accounts for a significant proportion of the total number of vehicles worldwide. In addition, vehicles with Hybrid transmission systems also account for a large number [I]. The common point of these 2 vehicles is to save internal combustion fuel and minimize harmful emissions emitted into the environment. Although internal combustion engines are still being developed, with the global air pollution situation, with emissions from internal combustion engines, inevitably, internal combustion vehicles will gradually be replaced. Therefore, car manufacturers now often equip their new models with Hybrid power trains, which take advantage of the fuel source from the internal combustion engine and use the electric fuel source from the battery unit. Even these companies have launched electric cars using fuel cells. Fuel cells can produce electricity continuously as long as fuel and oxygen are supplied [II]. Battery and fuel cells are now produced in quite a quantities and are popular to serve the world in general and for the automotive engineering technology industry in particular. Many different types have been fabricated and operationalized. However, they all have a fairly similar principle of operation; they consist of three adjacent segments: anode, electrolyte, and cathode. Fuel cells such as: proton exchange membrane fuel cells (PEMFCs) have low operating temperatures, continuous operation at high current densities, lightweight, compactness, low cost and

mass potential, fast start-up and suitable for intermittent operation [III]; Phosphoric acid fuel cells (PAFC) have a relatively high efficiency and excellent technical characteristics, but their widespread popularity in the market has slowed down due to economic issues [IV]; alkaline fuel cells (AFC) have made significant progress in replacing traditional liquid electrolyte alkaline fuel cells, and the performance of alkaline catalyst materials has seen remarkable advancements; however, achieving long-term stability remains a challenge [V]; Solid oxide fuel cells (SOFC) are being developed for various power generation applications, capable of efficiently generating electricity from different types of fuels for many power generation applications [VI]; molten carbonate fuel cells (MCFC) require a high operating temperature of 650°C (1200 °F). Among the mass-produced battery types, nickel-metal hybrid (Ni-MH) batteries and lithium-ion (Li-ion) batteries are two widely used and popular types in the automotive engineering technology industry worldwide. Over the past 25 years, commercial Li-ion batteries have continuously improved in terms of cost, lifespan, energy density, and other metrics. However, the increase in energy density, especially weight density, is quite limited. This leads many to believe that the application of EVs in the mass market will require the development of a completely new type of battery chemistry with the potential to achieve higher energy density than Li-ion, referred to as "beyond Li-ion" [VII]. Li-ion batteries are used in many lines of Hybrid vehicles. The principal shortcoming of lithium-ion batteries lies in their inclusion of a costly and relatively scarce component [VII]. Moreover, nickel-metal hydride (Ni-MH) batteries have ascended to prominence as the popular power storage paradigm for electric automobiles. Prominent automakers are presently promoting electric vehicles equipped with Ni-MH batteries for commercial deployment. Toyota recently launched the world's first commercial hybrid electric vehicle (HEV), the Toyota Prius, version is also equipped with a special Ni-MH battery [VIII].

Determining the optimal charging method for Ni-MH batteries to achieve the best average lifespan remains a challenge, as tests comparing different charging protocols do not yield clear results. Finally, unlike Ni-Cd batteries, Ni-MH batteries do not have clear signs of being fully charged (e.g., sudden voltage drop), requiring more complex charging control methods (based on time and temperature) to avoid overcharging that can damage the battery. Therefore, this paper primarily studies nickel-metal hybrid (Ni-MH) batteries operating in hybrid vehicles regarding performance, current, and state of charge.

#### II. Determine the basic parameters of Ni–MH battery

 $C_{pack}$ 

The research surveyed on Nickel–Metal Hydride (Ni-MH) batteries [IX, X] used in Hybrid cars, with the specifications presented in Table 1, is as follows:

Symbol Value Value **Symbol Symbol** Value Value Symbol 201.6 7.2 1.8 1.05  $m_{Module} \\$  $U_{\text{Module}}$ Upack  $P_{\text{Theory}}$ 

R

10

Table 1: Initial parameter values of Ni-MH batteries

6.5

The energy of the module in the battery [XI]:

28

L. K. T. Vo et al

 $N_{Module}$ 

$$E_{\text{Module}} = C_{\text{Module}} \times U_{\text{Module}} \tag{1}$$

After calculating the energy of one module in the battery, the researcher can determine the storage energy of the entire battery pack using equation (2) and the module-specific energy in equation (3).

Energy storage of the battery:

$$E_{\text{pack}} = N_{\text{Module}} \times E_{\text{Module}} \tag{2}$$

Specific energy for a Ni-MH module [IX]:

$$E_{Sp-Module} = \frac{U_{Module} \times C_{Module}}{m_{Module}}$$
 (3)

Battery power serves as a metric quantifying the quantum of energy dischargeable by the cell across a chronometric interval, as delineated in equation (4):

$$P_{Theory} = U_{Pack} \times I \tag{4}$$

Equation (5) elucidates that the efficacious power P deliverable by the battery to the load equates to its nominal output  $(V_{OC} \times I)$  diminished by the dissipation attributable to intrinsic resistance  $(R \times I^2)$  [I]. This power loss is unavoidable in any real power source with non-zero internal resistance. As intrinsic resistance burgeons, power dissipation intensifies, thereby curtailing the proficiency of energy conveyance to the recipient. Predicated upon equation (4) to determine  $V_{oc}$ ,  $P_{Loss}$  in equations (5) and (6).

$$P = (V_{OC} \times I) - R \times I^2 \tag{5}$$

The loss of power:

$$P_{Loss} = R \times I^2 \tag{6}$$

Based on the results in the study [XII, XIII], to determine the current in charging modes and charging efficiency, including:  $I_{batt(t)} = 6.5A$ ,  $I_{batt} = 0.65A$ ,  $v\grave{a}$   $\eta = 85\%$ .

The charging time:

$$t = \frac{\text{Battery capacity (mAh).120\%}}{\text{Charging speed (mA)}} \tag{7}$$

The equation for the charging state of the battery [XIV]:

$$SoC(t) = SoC_0 - \frac{1}{C_{\text{pack}}} \times \int_{t_0}^{1} I_{\text{batt}}(t) dt. 100$$
 (8)

In equation (8), the battery current  $I_{batt}(t)$  is defined as positive when discharging the battery; thus, the SoC level decreases over time, leading to the negative sign in the expression.

However, because in this model the charging current is defined as positive, the Coulomb Counting equation is rewritten with a plus sign to reflect the increase in State of Charge (SoC) during the charging process. The charging state equation can be applied to the time-varying I(t) using the Coulomb Count method presented in equation (9):

$$SoC(t) = SoC_0 + \frac{1}{C_{pack}} \times \int_{t_0}^{1} I_{batt}(t) dt. 100$$
 (9)

Effective current, which is the actual current that contributes to charging the battery after accounting for charging efficiency.

$$I_{ef} = I_{batt} \times \eta \tag{10}$$

Q is the charge (Ah) stored in the battery during a specific phase, usually the first phase, the constant current (CC) phase, followed by the constant voltage (CV) phase when the battery has reached a certain level of charge. It is calculated by multiplying the useful current by the time of that phase.

$$Q = I_{ef} \times \Delta_t \tag{11}$$

# III. Analysis results

Based on the preceding equations, the fundamental attributes of the Ni-MH batteries have been calculated and are illustrated in Table 2 below:

Symbol Value **Symbol** Value **Symbol** Value **Symbol** Value 46.8 202.34 12  $E_{\text{Module}}$  $V_{OC}$ 8.9  $t_{Standard}$ 1.3104 44.6 1.2 0.0008 Epack E<sub>Sp-Module</sub>  $P_{Loss}$  $t_{Fast}$ 

Table 2: Values of Ni-MH batteries

The power loss during power transmission is shown in Figure 1.

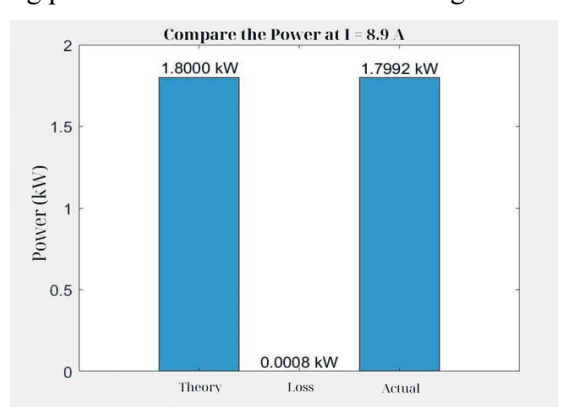


Fig. 1. Chart comparing theory power, loss power, and actual power

Based on the comparison results shown in Figure 1, when the current is 8.9 A, we can see the comparison between the theoretical power, actual power, and loss power. The theoretical power reaches 1.8 kW, which is the level of power that the system can achieve under perfect conditions, without any energy loss. However, in reality, the measured power is 1.7992 kW, slightly lower than the theoretical power. This difference is due to the loss of power, simulated as 0.0008 kW. Therefore, a modicum of energy dissipates amid the system's veritable functioning, causing the efficacious output to be inferior to its theoretical counterpart.

In fast charging mode (1.2 hours)

CC stage (0-0.8 hours, 6.5 A):

$$I_{ef 1} = 6.5 \times 0.85 = 5.525(A)$$
 $Q_1 = 5.525 \times 0.8 = 4.42 \text{ (Ah)}$ 
 $SoC_{(0-0.8h)} = \frac{4.42}{6.5} \times 100\% \approx 68\%$  (12)

CV stage (0.8-1 hour, 3.25 A):

$$I_{ef 2} = 3.25 \times 0.85 = 2.7625 \text{ (A)}$$
 $Q_2 = 2.7625 \times 0.2 = 0.5525 \text{ (Ah)}$ 
 $SoC_{(0.8-1h)} = 68 + \frac{0.5525}{6.5} \times 100\% \approx 76.5\%$  (13)

Protection stage (1-1.2 hours, 3.5 A):

$$I_{ef 3} = 3.5 \times 0.85 = 2.975 \text{ (A)}$$
 $Q_3 = 2.975 \times 0.2 = 0.595 \text{ (Ah)}$ 
 $SoC_{(1-1.2h)} = 76.5 + \frac{0.595}{6.5} \times 100\% \approx 85.7\%$  (14)

In standard charging mode (12 hours)

CC stage (0-8 hours, 0.65 A):

$$I_{ef} = 0.65 \times 0.85 = 0.5525 \text{ (A)}$$
 $Q_1 = 0.5525 \times 8 = 4.42 \text{ (Ah)}$ 
 $SoC_{(0-8h)} = \frac{4.42}{6.5} \times 100\% \approx 68\%$  (15)

CV stage (8-10 hours, 0.325 A):

$$I_{ef} = 0.325 \times 0.85 = 0.27625 \text{ (A)}$$

$$Q_2 = 0.27625 \times 2 = 0.5525 \text{ (Ah)}$$

$$SoC_{(8-10h)} = 68 + \frac{0.5525}{6.5} \times 100\% \approx 76.5\%$$
(16)

Protection stage (10-12 hours, 0.35 A):

$$I_{ef} = 0.35 \times 0.85 = 0.2975 \text{ (A)}$$

$$Q_3 = 0.2975 \times 2 = 0.595 \text{ (Ah)}$$

$$SoC_{(10-12h)} = 76.5 + \frac{0.595}{6.5} \times 100\% \approx 85.7\%$$
(17)

Total electric charge:

$$Q_{Total} = 4.42 + 0.5525 + 0.595 = 5.5675 \text{ (Ah)}$$
  
 $SoC_{(12h)} = \frac{5.5675}{6.5} \times 100 \approx 85.7 \%$  (18)

In Figure 2, both graphs show the difference between the actual and theoretical charging processes due to the charging efficiency  $\eta$  being less than 1. An inferior charging efficiency ( $\eta=0.85$ ) signifies that only a fraction of the imparted electrical energy is sequestered in the battery, with the surplus dissipated as thermal output or expended via parasitic reactions. This results in the actual SoC being always lower than the theoretical SoC at the same charging time.

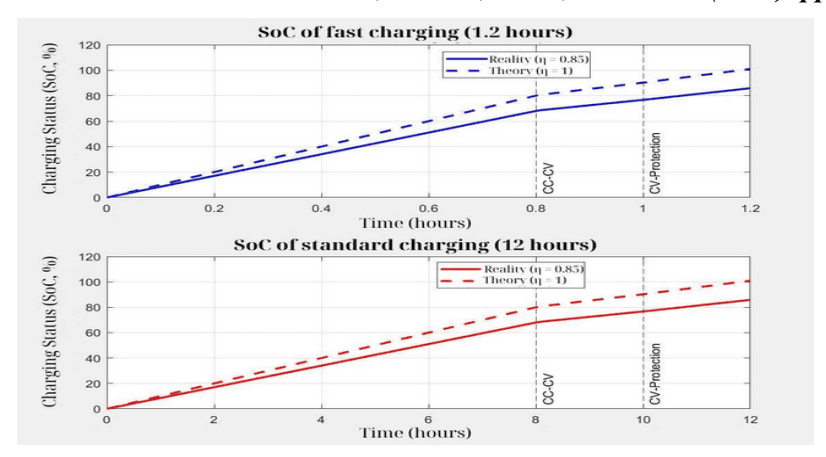


**Fig. 2.** State of Charge (SoC) of Ni-MH battery in fast charge and standard transfer mode

The simulation results in Figure 2 showed that fast charging reaches an equivalent SoC in significantly less time compared to standard charging. CC-CV stage: The transition from constant current to constant voltage occurs earlier in the fast charging process. Efficiency: Although the charging efficiency is assumed to be the same ( $\eta = 0.85$ ) for both methods, in reality, the fast charging efficiency may be lower due to the higher charging current causing greater thermal losses. Both charging methods have a constant voltage phase and may have intervention from the protection system to prevent overcharging and ensure the safety of the battery. Figure 2 illustrates scientifically how the charging state of a battery changes over time under two different charging methods (fast and standard), while also indicating the impact of non-theory charging efficiency and the stages of charge control (constant current, constant voltage, protection) on this process. Fast charging helps shorten charging time but can put more stress on the battery, while standard charging occurs more slowly and may extend the battery's lifespan.

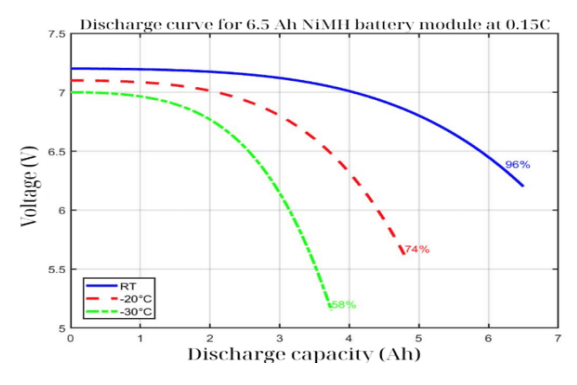


**Fig. 3.** The discharge curves of a 6.5 Ah prismatic NiMH battery module, obtained when discharging at a rate of 0.15 C and at different temperatures: room temperature (RT), -20 °C, and -30 °C [XV]

Figure 3 clearly illustrates the impact of temperature on the discharge capability of a NiMH battery module with a capacity of 6.5 Ah. When operating at room temperature, the battery demonstrates impressive discharge efficiency, reaching up to 96% of the

capacity claimed by the manufacturer, even when the discharge process occurs slowly (at a rate of 0.15 C). However, this efficiency drops significantly when the temperature decreases. At -20 °C and -30 °C, the battery can only provide 74% and 58% of its nominal capacity, respectively.

Research also indicates that the internal resistance of batteries increases significantly at low temperatures. For fully charged batteries (100% SoC), the internal resistance increases by 3.9 times at -25 °C and by 5.2 times at -30 °C compared to when operating at room temperature. The primary reason for this precipitous surge in here in the amplification of kinetic resistance at the anodes (negative electrode), which inexorably enervates the battery's aptitude for power conveyance.

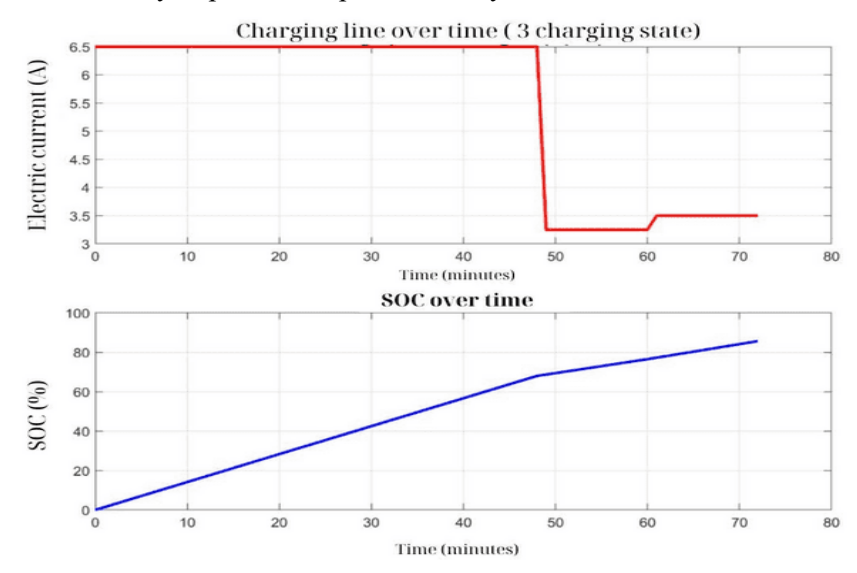


**Fig. 4.** Simulation of the charging current and state of charge (SoC) of the NiMH battery according to 3 states of fast charging: CC (0–0.8 h, 6.5 A), CV (0.8–1 h, 3.25 A), protection (1–1.2 h, 3.5 A)

The results in Figure 4 illustrate the charging current over time, starting at 6.5 A during the constant current (CC) state from 0 to 48 minutes, then decreasing to 3.25 A during the constant voltage (CV) state from 48 to 60 minutes, and maintaining at 3.5 A during the protection state from 60 to 72 minutes. The chart shows the increase in State of Charge (SoC) from 0% to about 85% after 72 minutes, reflecting the actual charging efficiency ( $\eta = 0.85$ ). This result shows that fast charging helps achieve a high State of Charge (SoC) in a short time, but high charging current can cause excessive heat loss, affecting battery lifespan, requiring improved thermal management to optimize the performance of Ni-MH batteries in hybrid vehicles. For fast charging of NiMH batteries, the current fluctuates from 3.25A to 6.5A. In contrast, for standard charging, the current will fluctuate from 0.325A to 0.65A through the stages, helping to reduce temperature and increase battery lifespan.

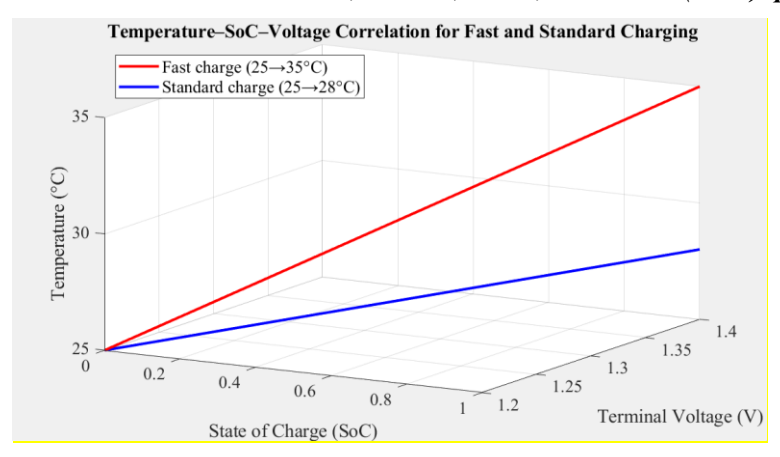


**Fig. 5.** Temperature - SoC - Voltage correlation for Ni-MH battery in fast and standard charging conditions

Figure 5 illustrates the interplay among temperature, state of charge (SoC), and terminal voltage in a Ni-MH battery module during both fast and standard charging conditions. The thermal progression is modeled after Ni-MH battery patterns ( $25 \rightarrow 35^{\circ}$ C for fast charge,  $25 \rightarrow 28^{\circ}$ C for standard charge). In fast-charging mode, the temperature escalates more swiftly owing to elevated current levels, which generate substantially more heat. This thermal escalation marginally elevates the internal resistance and induces a minor voltage decline at elevated SoC levels. Such an analysis underscores the critical need to integrate thermal effects within battery simulations to precisely forecast charging efficacy and performance across varying operational contexts, as explored in the referenced work [XVI].

#### IV. Conclusions

In this article, the authors investigated and surveyed the characteristics of the battery in Hybrid cars, specifically Ni-MH batteries. The study applied Matlab Simulink software to simulate factors related to the battery during use. The research results showed that the measured power of the Ni-MH batteries was only slightly lower than the theory power at 0.0008 kW; temperature affects the usability of the battery, specifically, the lower the temperature, the more the battery capacity percentage decreases; in addition, the higher the charging current, the more it affects the battery's lifespan, although the charging time is quick. Therefore, it is recommended that users of Hybrid vehicles use Ni-MH batteries when charging the battery with a current ranging from 3.25A to 6.5A. The paper can also be used as a research document on batteries for manufacturers and producers of Hybrid cars.

# **Conflict of Interest:**

There was no relevant conflict of interest regarding this paper.

#### References

- I. Buchmann I., Batteries I., in a Portable World: A Handbook on Rechargeable Batteries for Non-Engineers. Cadex Electronics Inc., 2012.
- II. Demirci, O., Taskin, S., Schaltz, E., and Acar Demirci, B. "Review of Battery State Estimation Methods for Electric Vehicles—Part I: SOC Estimation." Journal of Energy Storage, vol. 87, 2024, article 111435. 10.1016/j.est.2024.111435
- III. Dimauro, L. "Power Transmission Systems: From Traditional to Magnetic Gearboxes." 2021. PhD diss., Politecnico di Torino. IRIS Politecnico di Torino. https://iris.polito.it/retrieve/e384c434-246e-d4b2-e053-9f05fe0a1d67/PhDThesis Dimauro Luca.pdf
- IV. Ferriday, T. B., and Middleton, P. H. "Alkaline Fuel Cell Technology—A Review." International Journal of Hydrogen Energy, vol. 46, no. 35, 2021, pp. 18489-18510. 10.1016/j.ijhydene.2021.02.203
- V. Gifford, P., Adams, J., Corrigan, D., and Venkatesan, S. "Development of Advanced Nickel/Metal Hydride Batteries for Electric and Hybrid Vehicles." Journal of Power Sources, vol. 80, nos. 1-2, 1999, pp. 157-63. 10.1016/S0378-7753(99)00070-1
- VI. Jung-Ho, W. "Applications of Proton Exchange Membrane Fuel Cell Systems." Renewable and Sustainable Energy Reviews, vol. 11, no. 8, 2007, pp. 1720-38. 10.1016/j.rser.2006.01.005
- VII. Khan, M. M. R., Amin, M. K., and Chakraborty, N. "Advances and Prospects of Biodegradable Polymer Nanocomposites for Fuel Cell Applications." Biodegradable and Biocompatible Polymer Nanocomposites, edited by Deba Kumar Tripathy et al., Elsevier, 2023, pp. 599-637. 10.1016/B978-0-323-91696-7.00018-0
- VIII. Linden, D., and Reddy, T. B. Linden's Handbook of Batteries, Fourth Edition. McGraw-Hill, 2011, AccessEngineering.
- IX. Luntz, A. "Beyond Lithium-Ion Batteries." SLAC National Accelerator Laboratory, vol. 6, no. 2, 2015, pp. 224-313.
- X. Martínez-Sánchez, R., Molina-García, A., Mateo-Aroca, A., and Ramallo-González, A. P. "Evaluating a Nickel–Metal Hydride (NiMH) Battery Regeneration Patent Based on a Non-Intrusive and Unsupervised Prototype." Batteries, vol. 10, no. 11, 2024, article 402. 10.3390/batteries10110402
- XI. Madani, S. S., Ziebert, C., and Marzband, M. "Thermal Behavior Modeling of Lithium-Ion Batteries: A Comprehensive Review." Symmetry, vol. 15, no. 8, 2023, article 1597. 10.3390/sym15081597

- J. Mech. Cont.& Math. Sci., Vol.-20, No.-9, November (2025) pp 91-101
- XII. Noga, M., and Juda, Z. "The Application of NiMH Batteries in a Light-Duty Electric Vehicle." Technical Transactions, no. 1, 2019, pp. 197-222. 10.4467/2353737XCT.19.014.10054
- XIII. Nguyen, Q. T. "Solid Oxide Fuel Cell Technology—Features and Applications." Solid State Ionics, vols. 174, nos. 1-4, 2004, pp. 271-77. 10.1016/j.ssi.2004.07.042
- XIV. Pierozynski, B. "On the Low Temperature Performance of Nickel-Metal Hydride (NiMH) Batteries." International Journal of Electrochemical Science, vol. 6, 2011, pp. 860-66.
- XV. Quintero Pulido, D. F., Covrig, C.-F., and Bruchhausen, M. "On the Performance of Portable NiMH Batteries of General Use." Batteries, vol. 11, no. 1, 2025, article 30. 10.3390/batteries11010030
- XVI. Sammes, N., Bove, R., and Stahl, K. "Phosphoric Acid Fuel Cells: Fundamentals and Applications." Current Opinion in Solid State and Materials Science, vol. 8, no. 5, 2004, pp. 372-78. 10.1016/j.cossms.2005.01.001